Materials Research Bulletin 106 (2018) 371–378

Contents lists available at ScienceDirect

Materials Research Bulletin

journal homepage: www.elsevier.com/locate/matresbu

Impedance characteristics and PTCR effect in lead free $BaTi_{1-x}Sn_xO_3$ piezoceramics

Lakshmi Kola[a], Atal Bihari Swain[a], Martando Rath[a,b], M. S. Ramachandra Rao[a,b], P. Murugavel[a,*]

[a] Department of Physics, Indian Institute of Technology Madras, Chennai 600036, India
[b] Nano Functional Materials Technology Centre, Department of Physics, Indian Institute of Technology Madras, Chennai 600036, Tamil Nadu, India

ARTICLE INFO

Keywords:
Piezoelectric
Impedance
Relaxation
Ac conductivity
PTCR

ABSTRACT

$BaTi_{1-x}Sn_xO_3$ of compositions $x = 0.07$, 0.08, 0.09, 0.10 and 0.11 are synthesized to study their piezoelectric and impedance characteristics. The studies revealed that the composition $x = 0.08$ exhibits the maximum piezoelectric coefficient ($d_{33} = 296$ pC/N) and remnant polarization ($P_r = 6.92$ μC/cm^2) values. The impedance analysis showed that the depressed semi-circular arc observed in the Nyquist's plots gave evidence for the existence of non-Debye type relaxation behavior in the compounds. The impedance studies suggested a possible correlation between the d_{33} and microstructural properties. The activation energies extracted from ac conductivity plots strongly indicate the existence of defect dipole assisted conductivity mechanism in the samples. Notably, the samples displayed positive temperature coefficient of resistance (PTCR) just above their ferroelectric transition. The frequency dependent ac conductivity follows the Jonscher's universal power law. The dominant conduction mechanism in the samples is determined to be the small polaron hopping mechanism.

1. Introduction

During the last few decades, a significant progress in the field of piezoelectric materials has been achieved with regard to the study of lead-free compositions. The aim to study lead free compositions is to find potential alternatives for conventional but hazardous lead-based compounds [1,2]. Amongst the lead-free candidates, perovskite ferroelectrics are given preference because of their high piezoelectricity, giant dielectric constant and ease in synthesizing in stoichiometric form. In this regard, piezoceramics like $BaTiO_3$, $KNbO_3$, $KTaO_3$, $Na_{1/2}Bi_{1/2}TiO_3$, $K_{1/2}Bi_{1/2}TiO_3$, $Na_{0.5}K_{0.5}NbO_3$, $BiMnO_3$ and their derivatives are studied for the improvement in dielectric and piezoelectric properties [1–4].

Among them, Sn doped $BaTiO_3$ is reported to be a promising lead-free alternative with immense potential for electromechanical device applications. The compound $BaTi_{1-x}Sn_xO_3$ is reported to show a high piezocoefficient (d_{33}) of 697 pC/N and permittivity ~ 75,000 at quadruple point, where rhombohedral, orthorhombic, tetragonal and cubic phases coexist [5]. Note that the parent compound $BaTiO_3$ shows ferroelectric to paraelectric transition (T_C) at 120 °C where it undergoes tetragonal to cubic structural transition. This is followed by two interferroelectric transitions at 0 °C ($T_{T\text{-}O}$ - tetragonal to orthorhombic structural transition) and -90 °C ($T_{O\text{-}R}$ - orthorhombic to rhombohedral structural transition). Upon doping Sn on Ti-site, the detailed structural investigations reveal that the T_C shifts towards lower temperature, whereas both $T_{O\text{-}R}$ and $T_{T\text{-}O}$ shift towards higher temperatures [5–10]. The compounds exhibit pure ferroelectric character till $x < 0.2$ and with further increase in Sn content, a ferroelectric-to-relaxor crossover takes place [11].

Though $BaTi_{1-x}Sn_xO_3$ is reported to exhibit high d_{33} value, the value and composition at which it shows the maximum largely differs in literature mostly due to the difference in synthesis conditions [5,10]. For example, Yao et al. studied the piezoelectric properties of $BaTi_{1-x}Sn_xO_3$ for $x = 0$ to 0.15 and reported the highest d_{33} of 697 pC/N for $x = 0.11$ which is the morphotropic phase boundary for this compound [5]. On the other hand, Kalyani et al. studied the d_{33} variation for $x = 0$ to 0.11, with high d_{33} value (~ 425 pC/N) observed for at least three compositions such as $x = 0.02$, 0.04 and 0.08 which are well below the morphotropic phase boundary [10]. Also, the impedance spectroscopic studies which could bring a better understanding about the occurrence of high piezocoefficient in terms of the dielectric behavior of the material is also lacking in literature. Moreover, the studies on the conduction mechanisms in $BaTi_{1-x}Sn_xO_3$ are not yet reported. Keeping in view the available literature, we have carried out the detailed dielectric and conduction studies on the polycrystalline $BaTi_{1-x}Sn_xO_3$ samples synthesized by solid state method.

It is noteworthy to mention that ac conductivity studies revealed an interesting positive temperature coefficient of resistance (PTCR) over a

* Corresponding author.
E-mail address: muruga@iitm.ac.in (P. Murugavel).

https://doi.org/10.1016/j.materresbull.2018.06.021
Received 11 March 2018; Received in revised form 3 June 2018; Accepted 15 June 2018
Available online 18 June 2018

region of temperature in $BaTi_{1-x}Sn_xO_3$ which is otherwise observed only in donor doped $BaTiO_3$ [12]. Overall, the present work brings out a possible correlation among the microstructure, dielectric and piezoelectric properties in addition to PTCR effect which may provide direction to enhance these characteristics for suitable device applications.

2. Materials and methods

Polycrystalline $BaTi_{1-x}Sn_xO_3$ ceramic samples of composition (x = 0.07, 0.08, 0.09, 0.10 and 0.11) near its morphotropic phase boundary were synthesized by the conventional solid state reaction method using $BaCO_3$, TiO_2 and SnO_2 as precursors with purities higher than 99.9%. The stoichiometric amount of the precursors were homogeneously mixed in agate mortar and the powders were calcined at 1200 °C for 4 h. The calcined powders were ground again with binder (6 wt.% polyvinyl alcohol) and pelletized into circular disks of 8 mm diameter and 1 mm thickness using a uniaxial hydraulic press. The pellets were finally sintered at 1400 °C for 4 h in an ambient condition. The crystal structure of the samples was studied at room temperature using Bruker D8 Discover powder X-ray diffractometer. The microstructure of the samples was examined using F50 field emission scanning electron microscopy (FESEM) and the average grain size was calculated using the ImageJ software. The sintered samples were polished on both sides and silver paste was applied as an electrode for electrical measurements. The impedance measurements were carried out as a function of temperature (-30 °C to 300 °C) and frequency (100 Hz–10 MHz) by employing Novocontrol Technologies impedance analyzer. Polarization-electric field hysteresis loops at room temperature were recorded using Radiant Technologies Incorporation (RT6000S) ferroelectric loop tracer. The d_{33} was measured, on samples poled at 2.5 kV/mm for 30 min at 27 °C, using Piezo test d_{33} meter.

3. Results and discussions

3.1. Structural and morphological studies

The X-ray diffraction patterns (XRD) obtained on $BaTi_{1-x}Sn_xO_3$ (x = 0.07, 0.08, 0.09, 0.10 and 0.11) samples at 27 °C for 2θ ranging from 10° to 70° are shown in Fig. 1. The observed XRD patterns for all samples indicate the formation of pure perovskite phase. The absence of Sn, Ba and Ti rich secondary phases suggests the incorporation of Sn into the crystal system. Overall, the patterns are indexed to the tetragonal structure with P4mm space group in comparison with the JCPDS

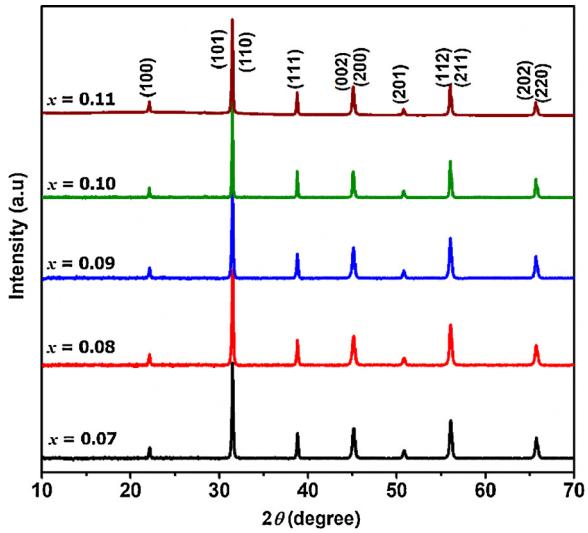

Fig. 1. The X-ray diffraction patterns of $BaTi_{1-x}Sn_xO_3$ (x = 0.07, 0.08, 0.09, 0.10 and 0.11) samples.

data. However, the evidence for orthorhombic phase can be seen for all compositions under study from the enlarged version of the XRD pattern for the 2θ angles 44.7–45.6° and 65.3–66.2° shown in Fig. 2. The systematic shift in peak position with respect to the doping concentration further reiterates the effective doping into the system.

To investigate the microstructure, the polished samples are thermally etched by annealing them at 1350 °C for 2 h. The thermally etched samples are subjected to SEM studies and the resultant images are shown in Fig. 3(a)–(d) for x = 0.07, 0.08, 0.09 and 0.10, respectively. The microstructures of all samples illustrate well grown grains distributed throughout the surface. To understand the grain size distribution among the samples, the histograms depicting the grain size variation are shown as an inset in the respective SEM images. Though it is inferred from the histogram that the samples show grain size varying from 1 to 60 μm, the average grain size is converging around 20 to 40 μm. The occurrence of such large grain sizes may be ascribed to the initial non-uniform grain size and high sintering temperature (1400 °C) adopted for densification. Note that among all samples, x = 0.08 exhibits uniform grains in the range of 5 to 25 μm. The density of the pellets measured by Archimedes' principle are found to be 5.69, 6.08, 5.84, 6.07, and 6.04 g/cm^3 for x = 0.07, 0.08, 0.09, 0.10 and 0.11, respectively.

3.2. Ferroelectric and piezoelectric studies

To study the ferroelectric properties, the polarization (P) is measured as a function of electric field (E) at 27 °C under 4 Hz and the results are plotted in Fig. 4(a) for all samples. The ferroelectric state of the samples are confirmed from the well saturated P-E hysteresis loops. To understand the compositional variation of ferroelectric characteristics, the remnant polarization (P_r) inferred from the enlarged version of the plots (shown in the inset of Fig. 4(a)) is plotted against composition in Fig. 4(b) along with the respective d_{33} values. Note that the P_r initially increases with a maximum value of 6.92 μC/cm^2 observed for x = 0.08, and thereafter shows decreasing trend with increase in x. The values are in agreement with the literature [13,14]. Interestingly, the d_{33} also shows similar trend with a maximum value of 296 pC/N for x = 0.08 composition. The reason for different maximum values of d_{33} obtained by other authors for significantly differing concentrations is the varying synthesis process and conditions used. It should be noted that in the present work, the samples have been prepared through grinding by mortar and pestle unlike the ball milling process widely used in literature. Slimmer P-E loops along with decrease in P_r and d_{33} for higher Sn doped compound could be attributed to the compound going towards relaxor-like behavior [11].

3.3. Dielectric studies

To understand the dielectric properties of the samples, the temperature (T) dependent real part of dielectric permittivity (ε') is measured from 100 Hz to 10 MHz and the results are plotted in Fig. 5. The Sn doped samples exhibit high permittivity and low loss tangent (not shown in the figure) which indicate good dielectric quality of these samples. The plot in Fig. 5(a) for x = 0.07 reveals two distinct anomalies at 40 °C and 14 °C along with the T_C at 71 °C. The two anomalies can be correlated to the reported structural phase transitions such as $T_{T\text{-}O}$ and $T_{O\text{-}R}$ along with the transition from tetragonal to cubic phase at T_C [13]. However, with increase in Sn doping both $T_{T\text{-}O}$ and $T_{O\text{-}R}$ shift towards higher temperature, whereas the T_C follows the reverse trend [13]. At x = 0.10 and 0.11, these transitions merge together and thereby broaden the T_C.

To analyze it further, the first derivatives of ε'versus T plots at 100 Hz are shown in Fig. 6 for all samples. The figure reveals anomalies at three different structural transitions and their variation with composition. The signature of broad transition at T_C is visible for x = 0.11. The dielectric data indicate that the compound x = 0.07 exhibits